DOI: 10.1002/ejoc.201000221

1,4,7,10-Tetraisoalkyltetracenes: Tuning of Solid-State Optical Properties and Fluorescence Quantum Yields by Peripheral Modulation

Chitoshi Kitamura,*[a] Hideki Tsukuda,[a] Akio Yoneda,[a] Takeshi Kawase,[a] Takashi Kobayashi,[b] and Hiroyoshi Naito[b]

Keywords: Oligoacenes / Substituent effects / Crystallochromy / Fluorescence / Absorption

We have synthesized 1,4,7,10-tetraisoalkyltetracenes from a 2,6-naphthodiyne precursor and 2,5-diisoalkylfurans as the starting materials (isoalkyl: isopropyl, isobutyl, and isopentyl). The tetracene molecules exhibited crystallochromy: The solid-state colors of the isopropyl, isobutyl, and isopentyl derivatives were yellow, red, and orange-yellow, respectively. In contrast, there were no marked differences in the optical properties of these compounds in solution. The isopropyl derivative exhibited the highest fluorescence quantum yield in the solid state of 0.90 in the series of alkylated tetracenes. X-ray analysis revealed that there were significant structural differences in alkyl conformation and crystal packing. The crystallochromy effects are derived from the unique crystal-packing patterns. The fluorescence quantum yields in the solid state probably depend on the relative positional relationship of the nearest neighboring molecules in one column as well as the crystal rigidity.

Introduction

Oligoacenes, particularly tetracene and pentacene, have attracted considerable attention in recent years for their electronic properties as organic semiconducting devices, such as organic field-effect transistors (OFETs), organic light-emitting diodes (OLEDs), and photovoltaic cells.[1] However, they suffer from some disadvantages, such as their low solubility in solution, instability in air, and poor thin-film morphologies, which limit their practical applications in low-cost device fabrication. Therefore many groups have increasingly performed acene functionalizations and reported various substituted oligoacenes.[2]

We recently prepared a series of linear alkyl-substituted tetracenes[3] (**1a–f**; Scheme 1). We then elucidated the effects of their linear alkyl side-chains on packing patterns and solid-state optical properties. The length of the alkyl side-chain was critical for creating the differences in alkyl conformation, molecular shape, packing pattern, and solid-state photophysical properties observed between the different alkyl-substituted tetracenes. Interestingly, the isolated solids exhibited colors varying from yellow to red (yellow: **1b** and **1d**; orange: **1a**, **1c**, and **1e**; red: another **1d** and **1f**), that is, crystallochromy,[4] an effect found for the first time among acenes. Furthermore, the fluorescence quantum yields in their powder forms were low to moderate (Φ_F = 0.13–0.40). Their solid-state emission efficiencies seemed unsatisfactory. The above study demonstrated that in the solid state, the alkyl side-chain could function not only as a spacer but also adjust the mutual positional relationship of the tetracene moieties. We then noticed the importance of the alkyl side-chain as a facile tool for controlling the photophysical properties in the solid state. Organic materials exhibiting highly intense emissions in the solid state have recently received considerable interest because molecules with high absolute quantum yields are quite limited.[5–14] Although several approaches, such as substituent protection,[5] π–π stacking protection,[6–8] intramolecular charge-transfer transition,[9] aggregation-induced emission,[10,11] and modulating molecular arrangements,[12–14] have been reported, molecular design to control solid-state fluorescence is not fully understood. To develop new tetracenes with high emission efficiencies, we thought to introduce isoalkyl groups as branched alkyl side-chains instead of linear alkyl groups. We expected that the effects of the bulkiness and shape of the isoalkyl groups might induce intermolecular separation between neighboring molecules as well as reduction of concentration quenching. Herein we report the

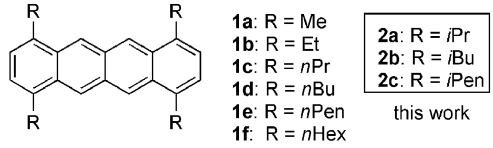

Scheme 1. Chemical structures of alkyl-substituted tetracenes.

[a] Department of Materials Science and Chemistry, University of Hyogo,
2167 Shosha, Himeji, Hyogo 671-2280, Japan
Fax: +81-79-267-4888
E-mail: kitamura@eng.u-hyogo.ac.jp
[b] Department of Physics and Electronics, Osaka Prefecture University,
1-1 Gakuen-cho, Naka-ku, Sakai, Osaka 599-8531, Japan

Supporting information for this article is available on the WWW under http://dx.doi.org/10.1002/ejoc.201000221.

solid-state optical properties and X-ray analysis of isoalkyl-substituted tetracenes **2a**–**c** bearing isopropyl, isobutyl, or isopentyl groups at the 1-, 4-, 7-, and 11-positions.

Results and Discussion

Synthesis of 1,4,7,10-Tetraisoalkyltetracenes

We prepared tetracenes **2a**–**c** by our recently reported procedure using 2,5-dialkylfurans and 2,6-napthodiyne precursor **5**.[3] 2,5-Diisobutylfuran (**4b**) and 2,5-diisopentylfuran (**4c**) were easily prepared by nucleophilic substitution reaction of 2,5-dilithiated furan with the corresponding alkyl halides. However, 2,5-diisopropylfuran (**4a**) could not be obtained by this method. Therefore we developed a new synthetic strategy (Scheme 2). Carbonyl addition of 2,5-dilithiated furan to acetone gave furan dialcohol **3**, which was readily hydrogenated to afford 2,5-diisopropylfuran (**4a**) in high yield. Reaction of the 2,6-naphthodiyne synthon, in situ generated from **5**, with furan **4a** in the presence of KF and 18-crown-6 provided Diels–Alder adduct **6a**. Finally, hydrogenation and subsequent acid-mediated dehydration produced tetracene **2a**. Tetracenes **2b** and **2c** were also prepared by the same procedure. Tetracenes **2a**, **2b**, and **2c** were isolated as yellow, red, and orange-yellow solids, respectively,[15] and were soluble in common organic solvents such as hexane and chloroform. Although the three tetracenes **2a**–**c** showed high air stability in the solid state, their solutions were unstable in the presence of both light and air.

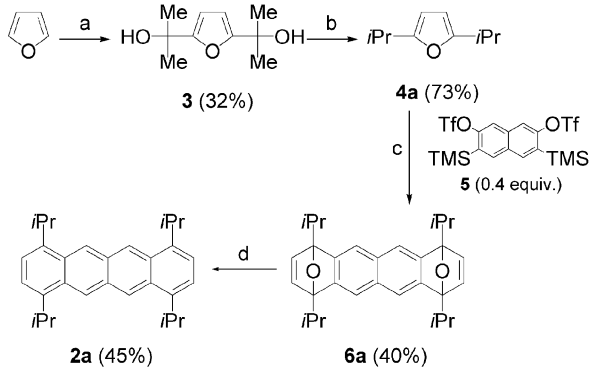

Scheme 2. Reagents and conditions: (a) 1. TMEDA (2.2 equiv.), *n*BuLi (2.4 equiv.), hexane, reflux, 1 h; 2. acetone (3.0 equiv.), THF, 0 °C to room temp. 17 h; (b) H_2, 10% Pd/C, CH_2Cl_2, room temp., 4 h; (c) KF (1.4 equiv.), 18-crown-6 (1.2 equiv.), THF, room temp., 18 h; (d) 1. H_2, 10% Pd/C, EtOH, room temp., 6 h; 2. concd. HCl/Ac_2O (1:5), room temp., 1 h.

Absorption and Fluorescence Spectra

UV/Vis absorption and fluorescence spectra reveal that there are no remarkable differences in the optical properties of **2a**–**c** in solution (Figure 1 and Table 1). These compounds show small Stokes shifts (13–14 nm). In addition, the quantum yields in hexane are low and identical (Φ_F = 0.11–0.12). These results can be explained by the following hypotheses: (1) the electronic effects of the isoalkyl substituents are the same regardless of their length and shape and (2) the molecules exist in a practically monodispersed state in dilute solution.

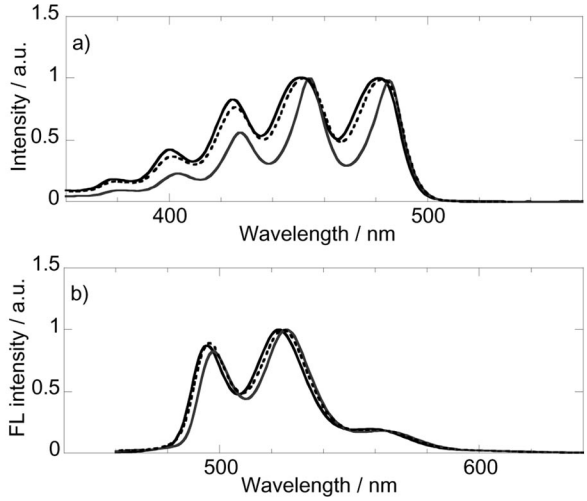

Figure 1. a) Absorption and b) fluorescence spectra of **2a** (solid line), **2b** (gray line), and **2c** (dashed line) in hexane.

Table 1. UV/Vis absorption and fluorescence properties of **2a**–**c** in hexane.

	Absorption λ_{max}[a] [nm] [log (ε/M^{-1} cm^{-1}]	Fluorescence λ_{em}[b] [nm]	Φ_F[c]
2a	425 [3.56], 451 [3.65], 481 [3.65]	495, 523, 539	0.12
2b	427 [3.66], 454 [3.91], 485 [3.91]	498, 526, 562	0.11
2c	426 [3.54], 452 [3.65], 482 [3.65]	496, 524, 560	0.11

[a] Peaks based on 0→0, 0→1, and 0→2 transitions. [b] Excited at 365 nm. [c] Fluorescence quantum yields were determined by using 9,10-diphenylanthracene as the standard.

On the other hand, significant differences in both the solid-state absorption (Kubelka–Munk) spectra of diluted KBr pellets and the fluorescence of the powder forms were observed (Figure 2 and Table 2). Their absorption spectra in the solid state (Figure 2, a) are characterized by different structured bands, which reflect crystallochromy effects, somewhat different behavior to that observed with the linear alkyl side-chain derivatives. The longest wavelength absorption maxima and absorption edges in the solid state are redshifted compared with those in solution, which indicates the presence of intermolecular interactions between the chromophores. The order of increase of both the longest wavelength absorption maxima and the absorption edges (**2a** < **2c** < **2b**) correlates well with that of the solid-state colors (isopropyl **2a**: yellow; isopentyl **2c**: orange-yellow; isobutyl **2b**: red). Their colors have little relevance to those of the corresponding linear alkyl derivatives (propyl **1c**:

orange; butyl **1a**: yellow and red; pentyl **1e**: orange), which suggests significantly different packing patterns in comparison with the linear alkyl derivatives.

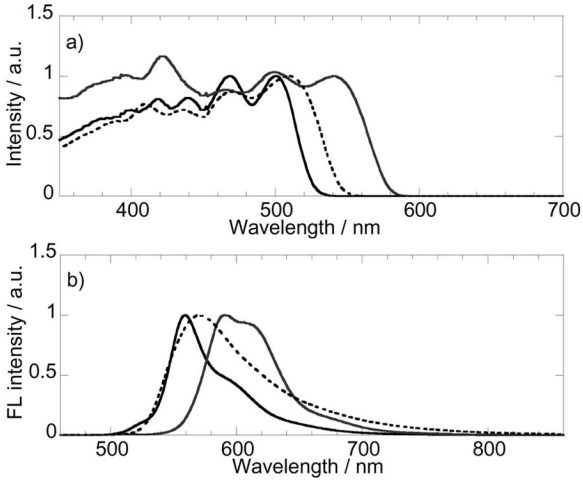

Figure 2. a) Kubelka–Munk spectra in diluted KBr pellets and b) fluorescence spectra in hexane of **2a** (solid line), **2b** (gray line), and **2c** (dashed line).

Table 2. UV/Vis absorption and fluorescence properties of **2a**–**c** in the solid state.

	Absorption[a]		Fluorescence[b]	
	λ_{max} [nm]	λ_{edge} [nm]	λ_{em}[c] [nm]	Φ_F[d]
2a	500	535	560	0.90
2b	541	584	590	0.42
2c	509	554	569	0.18

[a] Kubelka–Munk spectra of the diluted KBR pellet. [b] Excited at 325 nm. [c] Maximum peak. [d] Absolute quantum yield in the powder form.

The solid-state fluorescence spectra of the powder forms of **2a**–**c** (Figure 2, b) exhibit the following fairly complicated spectral features: (1) **2a** shows a sharp fluorescence spectrum with a fluorescence maximum at 560 nm and a shoulder peak at around 600 nm; (2) **2c** exhibits one broad band with the peak located at 569 nm; (3) **2b** exhibits two bands (a fluorescence maximum at 590 nm and a shoulder peak at around 620 nm), which are more redshifted than the peaks of **2a** and **2c**. The Stokes shifts are 60, 49, and 60 nm for **2a**, **2b**, and **2c**, respectively. Surprisingly, the absolute quantum yields (Φ_F) of **2a**–**c** vary over a much wider range (Φ_F = 0.18–0.90) than those of the linear alkyl derivatives **1a**–**f** (Φ_F = 0.13–0.40). In particular, **2a** exhibits the largest quantum yield (Φ_F = 0.90) of any tetracene derivative ever reported. Furthermore, even the Φ_F value of **2b** is 0.42, which is comparable to the maximum value among **1a**–**f** (Φ_F = 0.40). The order of decrease of the solid-state quantum efficiencies (**2a** > **2b** > **2c**) is most likely correlated with the length of the isoalkyl side-chains.

Crystal Structures

To elucidate the characteristic optical properties of **2a**–**c** in the solid state, we determined their crystal structures (Figure 3). The molecules have a crystallographic center of symmetry, which indicates that half of the molecular formula unit is independent. The tetracene rings in the crystals of **2a**–**c** are all essentially planar. However, the isoalkyl groups are characterized by alkyl conformations that significantly vary in length (Figure 3). For **2b**, all four substituent groups as a whole give rise to a *gauche* conformation in which the two isobutyl groups at the 1- and 4-positions extend upward and the others at the 7- and 10-positions extend downward. As for **2a** and **2c**, although the conformations of the four substituent groups look similar, there are small differences in the directions of the two terminal methyl groups of the isoalkyl groups. Thus, two terminal methyl groups of the two isopropyl groups at the 1- and 4-positions point upward and two methyl groups of the other two isopropyl groups at the 7- and 10-positions point upward, whereas two terminal methyl groups of two isopentyl groups at the 1- and 10-positions point downward and two methyl groups of the other two isopentyl groups at the 4- and 7-positions point upward.

Time-dependent density functional theory (TD-DFT) calculations performed by using the B3LYP/6-31G* method on the geometry obtained by X-ray analysis showed the

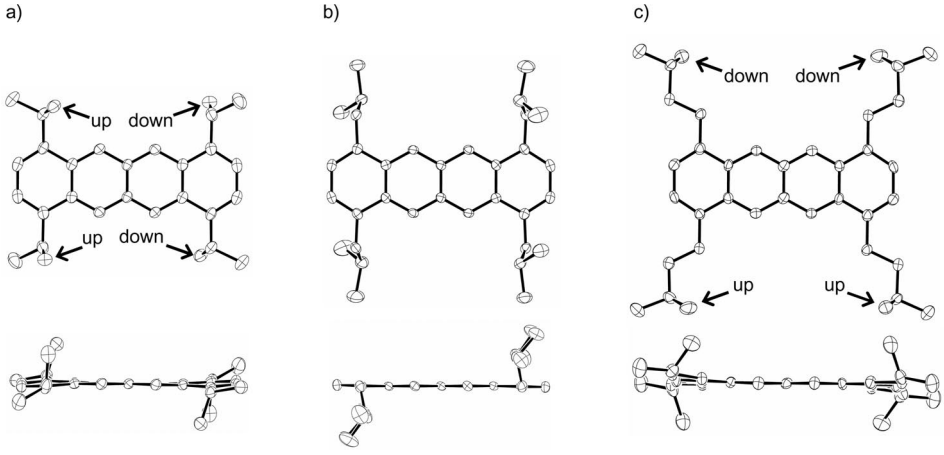

Figure 3. Molecular structures of a) **2a**, b) **2b**, and c) **2c**, showing top view (upper) and side view (lower).

lowest-energy absorption bands at single molecular levels of 492, 496, and 469 nm for **2a**, **2b**, and **2c**, respectively.[16] These values are in agreement with the absorption maxima in solution. However, the calculations did not agree with the absorption maxima of the actual solids, which indicates that some corrections based on intermolecular interactions such as exciton coupling were required to properly estimate the color of the solids.

The considerable differences in the alkyl conformations probably lead to the unique crystal-packing structures of **2a**–**c**. We observed drastically different stacking patterns of two neighboring molecules in one column (Figure 4). Molecule **2b** exhibits a large π overlap, which would be a major factor contributing to the redshifts observed in the absorption and emission spectra in the solid state. In molecule **2a**, there is a slight π overlap. In contrast, there is no π overlap in molecule **2c**. We then surveyed the geometric parameters of the tetracene slip distance (*s*), interplanar spacing (*d*), longitudinal shift (*l*), and transverse shift (*t*) between two neighboring tetracene units (Table 3). Although the *d* distance is close to 3.5 Å for all three systems, which is a typical interplanar stacking spacing, **2a**–**c** exhibit a wide variety of *s*, *l*, and *t* distances. The *s* distances are 6.34, 5.27, and 4.81 Å for **2a**, **2b**, and **2c**, respectively, which probably reflects the degree of bulkiness of the substituent groups. The *l* and *t* shifts are also significantly different. We found that the larger the *l* shift, the larger the quantum yield. Thus, **2a** has the largest *l* shift (4.95 Å) and the largest quantum yield (Φ_F = 0.90), **2b** has the second largest values (3.91 Å and Φ_F = 0.42), and **2c** has the lowest (0.58 Å and Φ_F = 0.18).

Table 3. Geometric parameters between two neighboring molecules of **2a**–**c**.

	s[a] [Å]	d[b] [Å]	l[c] [Å]	t[d] [Å]
2a	6.34	3.46	4.95	1.90
2b	5.27	3.46	3.91	0.70
2c	4.81	3.55	0.58	3.19

[a] Slip distance. [b] Interplanar spacing. [c] Longitudinal shift. [d] Transverse shift.

The packing patterns of **2a**–**c** are completely different to each other (Figure 5). They are also completely different to those of the linear alkyl-substituted tetracenes **1a**–**f**. We believe that the packing patterns depend upon the balance of intermolecular interactions between aromatic rings, such as the face-to-face and edge-to-face interactions, and the self-assembling capabilities of the alkyl side-chains. Molecules **2a** and **2c** appear to be stacked in herringbone-like structures. The interplanar tilt angles between tetracene rings in two adjacent columns are 66.9 and 155.0° for **2a** and **2c**, respectively. In contrast, the tetracene rings in **2b** adopt a slipped-parallel arrangement of stacked molecular sheets. In the crystal of **2a**, the nearest center-to-center distances between the tetracene rings in three neighboring columns are 9.67, 9.90, and 13.80 Å. On the other hand, **2b** has nearest center-to-center distances of 11.15, 11.93, and 15.66 Å, and **2c** has distances of 10.97, 16.12, and 16.12 Å. In consideration of the structural information described previously, we attempted to evaluate the intermolecular interactions by using the simple point–dipole molecular exciton model of Kasha[17] as we had already analyzed the exciton displacement energy between nearest-neighbor molecules in **1a**–**f**.[3b] However, we could not obtain a reasonable energy shift value for **2a** (0.0025 eV), although values of 0.0195 and –0.0150 eV were obtained for **2b** and **2c**, respectively. This suggests that the model used to consider only nearest-neighbor molecules for intermolecular interactions may have limitations for molecules possessing an extremely high fluorescence quantum yield in the solid state. To understand crystallochromy accurately, a higher level of theory dealing with intermolecular interactions would be necessary. We attributed the observed crystallochromy to the unique packing patterns, which lead to the inherent intermolecular interactions in the solid state.

We considered the fluorescence quantum yields in the solid state from the view point of crystal packing. In the crystal of **2a**, molecules are slightly further away from neighboring molecules in one column (i.e., longer *s* and *l* distances), although the center-to-center distances between adjacent columns are relatively short compared with those of **2b** and **2c**. In these circumstances, the distance between neighboring molecules in one column should be one of the most dominant factors determining the fluorescence quantum yield in the solid state. Thus, a longer distance between neighboring molecules in one column can interrupt concentration quenching leading to a higher quantum yield in the solid state. In addition, crystal rigidity is another possible factor.[13b] The existence of longer isoalkyl groups should reduce crystal rigidity because of an abundance of flexible linear methylene chains, which would then lead to not only

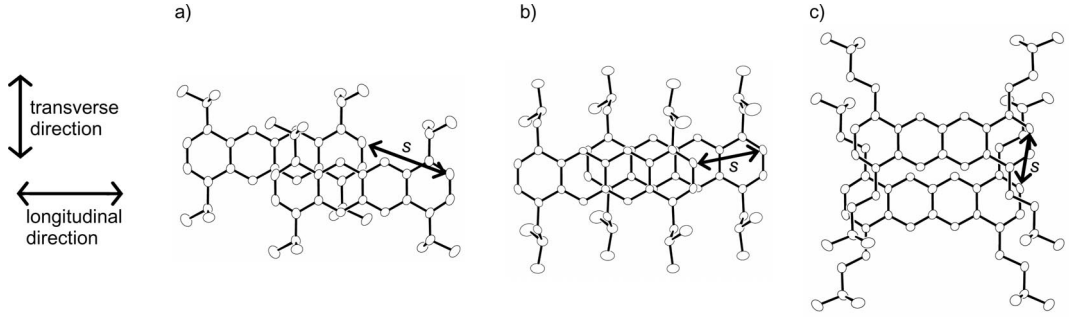

Figure 4. Stacking patterns of two neighboring molecules of a) **2a**, b) **2b**, and c) **2c**, where *s* denotes the slip distance.

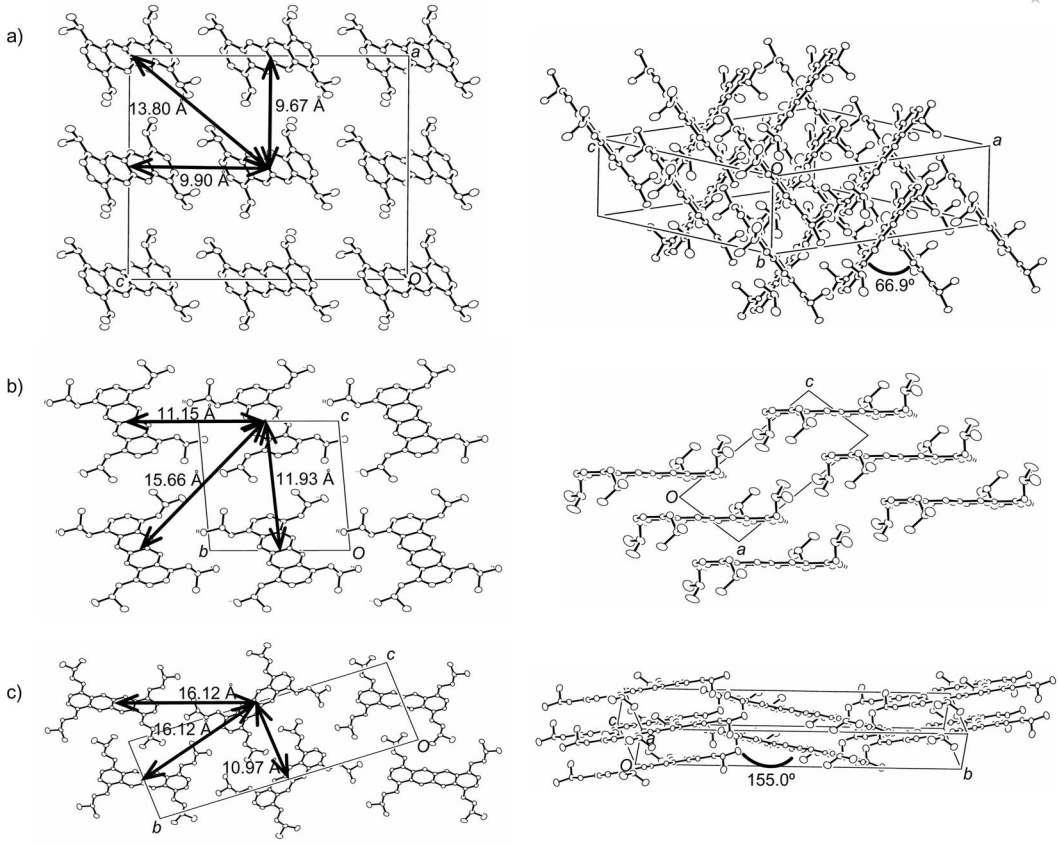

Figure 5. Packing diagrams of a) **2a**, b) **2b**, and c) **2c** showing views along the stacking direction (left) and from the side (right).

an enhancement of nonradiative decay of the excited states but also to the reduction of the quantum yield. Therefore we concluded that both the relative positional relationship between neighboring tetracene units and the crystal rigidity derived from the peripheral substituents are critical factors for controlling the solid-state fluorescence quantum yield.

Conclusions

In this work we prepared three new tetracenes possessing different isoalkyl groups at the 1-, 4-, 7-, and 10-positions and investigated their solid-state optical properties and crystal structures. Both the crystallochromy and solid-state fluorescence quantum yields were easily modulated by peripheral isoalkyl substitution. In particular, molecule **2a**, which bears bulky isopropyl groups, exhibits the highest quantum yield ever reported for tetracenes. Both the relative positional relationship between neighboring tetracene units and the rigidity of the crystal packing probably lead to the enhancement of the quantum yields. Their crystal structures demonstrate complicated conformations of isoalkyl groups and different stacking patterns between neighboring molecules and packing patterns in the crystals. These results will have a significant effect on the molecular design of other alkylated chromophores and fluorophores in the solid state.

Experimental Section

General: All reagents were commercially available and used without further purification. Solvents used in syntheses were purified by standard methods. Column chromatography was performed on Wako silica gel C-300 (45–75 μm). Melting points were measured with a Yanaco melting-point apparatus. ^{1}H and ^{13}C NMR spectra were measured with a Bruker-Biospin DRX500 FT spectrometer. EI-MS spectra were obtained at 70 eV with a Shimadzu GC–MS QP5050A instrument. Elemental analyses were carried out with a Yanaco MT-5 CHN instrument. Absorption and fluorescence spectra in solution were recorded with Hitachi U3500 and F2500 spectrophotometers, respectively. Fluorescence yields (Φ_F) in solution were determined with 9,10-diphenylanthracene (Φ_F = 0.86)[18] in cyclohexane as the standard. Kubelka–Munk spectra were measured with a Hitachi U3010 spectrophotometer with a Φ60 integrating sphere attachment. Fluorescence spectra in the solid state were recorded using a Hamamatsu Photonics PMA11 calibrated optical multichannel analyzer (λ_{ex} = 325 nm) and the absolute quantum yields (Φ_F) were determined with a Labsphere IS-040-SF integrating sphere. TD-DFT calculations were carried out by using the B3LYP/6-31G* method with the Gaussian 03 program package.[19]

2,5-Diisopropylfuran (4a): A 1.6 M solution of *n*BuLi in hexane (20 mL, 32.0 mmol) was added slowly to an ice-cooled mixture of furan (1.0 mL, 13.8 mmol) and TMEDA (5.0 mL, 30.2 mmol) and the mixture was heated at reflux for 1 h. During heating, the mixture changed to a brown suspension. The mixture was allowed to cool to room temperature and then further cooled with an ice bath.

A solution of acetone (3.1 mL, 42.2 mmol) in THF (10 mL) was added dropwise to the ice-cooled mixture. The mixture was then stirred at reflux for 17 h. After cooling to room temperature, the mixture was quenched with water. The crude product was extracted with AcOEt, washed with brine, and dried with Na_2SO_4. After evaporation of the solvents, the residue was subjected to column chromatography ($CHCl_3$/AcOEt = 1:1) on silica gel to give **3** (817 mg, 32%) as a yellow solid (m.p. 55–58 °C). ^{1}H NMR (500 MHz, $CDCl_3$): δ = 1.57 (s, 12 H, CH_3), 2.52 (br. s, 2 H, OH), 6.07 (s, 2 H, Ar-H) ppm. ^{13}C NMR (126 MHz, $CDCl_3$): δ = 28.47, 68.64, 103.95, 158.97 ppm.

A solution of **3** (817 mg, 4.44 mmol) in CH_2Cl_2 (25 mL) was hydrogenated over 10% Pd/C (59 mg) under atmospheric pressure at room temperature for 6 h. The catalyst was removed by filtration and the filtrate was concentrated under reduced pressure. Column chromatography (hexane) on silica gel afforded **4a** (399 mg, 73%) as a yellow oil, which was used in the next reaction without further purification. ^{1}H NMR (500 MHz, $CDCl_3$): δ = 1.22 [d, J = 6.8 Hz, 12 H, $CH(CH_3)_2$], 2.89 [sept, J = 6.8 Hz, 2 H, $CH(CH_3)_2$], 5.83 (s, 2 H, Ar-H) ppm. ^{13}C NMR (126 MHz, $CDCl_3$): δ = 21.11, 27.79, 102.57, 159.78 ppm.

2,5-Diisobutylfuran (4b): This compound was synthesized following our recently reported procedure.[3b] A 1.6 M solution of *n*BuLi in hexane (20 mL, 32.0 mmol) was added slowly to an ice-cooled mixture of furan (1.0 mL, 13.8 mmol) and TMEDA (5.0 mL, 30.2 mmol) and the mixture was heated at reflux for 1 h. During heating, the mixture changed to a brown suspension. The mixture was allowed to cool to room temperature and then further cooled with an ice bath. A solution of isobutyl bromide (4.6 mL, 42.0 mmol) in THF (10 mL) was added dropwise to the ice-cooled mixture. The mixture was stirred at room temperature for 17 h. After quenching with water, the crude product was extracted with Et_2O, washed with brine, and dried with Na_2SO_4. After evaporation of the solvents, the residue was subjected to column chromatography ($CHCl_3$/hexane = 1:1) on silica gel and dried under vacuum with mild heating (50 °C) to remove unreacted isobutyl bromide and monosubstituted furan. The disubstituted furan **4b** (1.05 g, 42%) was obtained as a yellow oil and used in the next reaction without further purification. ^{1}H NMR (500 MHz, $CDCl_3$): δ = 0.91 [d, J = 6.7 Hz, 12 H, $CH_2CH(CH_3)_2$], 1.90–1.95 [m, 4 H, $CH_2CH(CH_3)_2$], 2.42 [d, J = 7.1 Hz, 2 H, $CH_2CH(CH_3)_2$], 5.83 (s, 2 H, Ar-H) ppm. ^{13}C NMR (126 MHz, $CDCl_3$): δ = 22.31, 28.02, 37.30, 106.00, 153.62 ppm.

2,5-Diisopentylfuran (4c): This compound was synthesized by the same procedure as described above for **4b** except for the use of isopentyl bromide (5.3 mL, 41.4 mmol) instead of isobutyl bromide; yield 928 mg (43%). ^{1}H NMR (500 MHz, $CDCl_3$): δ = 0.91 [d, J = 6.6 Hz, 12 H, $CH_2CH_2CH(CH_3)_2$], 1.48–1.53 [m, 4 H, $CH_2CH_2CH(CH_3)_2$], 1.56–1.59 [m, 2 H, $CH_2CH_2CH(CH_3)_2$], 2.56 [t, J = 7.9 Hz, 4 H, $CH_2CH_2CH(CH_3)_2$], 5.82 (s, 2 H, Ar-H) ppm. ^{13}C NMR (126 MHz, $CDCl_3$): δ = 22.41, 26.04, 27.62, 37.11, 104.69, 154.63 ppm.

1,4,7,10-Tetraisopropyltetracene (2a): KF (324 mg, 5.57 mmol) was added to a solution of bis(aryne) precursor **5**[3b] (868 mg, 1.53 mmol), dialkylfuran **4a** (487 mg, 3.97 mmol), and 18-crown-6 (1.31 g, 4.95 mmol) in THF (50 mL). The mixture was stirred at room temperature for 18 h. Water was added and the resulting mixture was extracted with $CHCl_3$. The combined organic layer was washed with brine and dried with Na_2SO_4. After removal of the solvents the residue was purified by column chromatography ($CHCl_3$/hexane = 1:1) to afford a mixture of *syn* and *anti* isomers of **6a** (234 mg, 36%) as a yellow solid (m.p. 122–125 °C). ^{1}H NMR (500 MHz, $CDCl_3$): δ = 1.20–1.27 [m, 24 H, $CH(CH_3)_2$], 2.63–2.69 [m, 4 H, $CH(CH_3)_2$], 6.76 (s, 4 H, 2-H, 3-H, 8-H, 9-H), 7.38 (s, 4 H, 5-H, 6-H, 11-H, 12-H) ppm. ^{13}C NMR (126 MHz, $CDCl_3$): δ = 18.15, 18.39, 27.97, 94.61, 118.30, 128.91, 143.92, 149.02 ppm.

Because **6a** was apt to decompose on standing at room temp., it was used in the next reaction as soon as possible. A solution of **6a** (234 mg, 0.55 mmol) in EtOH (55 mL) was hydrogenated over 10% Pd/C (46 mg) under atmospheric pressure at room temperature for 4 h. The catalyst was removed by filtration and the filtrate was concentrated under reduced pressure. A cold solution of concd. HCl (1 mL) and Ac_2O (5 mL) at 0 °C was added to the residue and the mixture was stirred at room temperature for 1 h. Water was added and the resulting mixture was extracted with $CHCl_3$. The combined organic layer was washed with brine and dried with Na_2SO_4. After removal of the solvents, column chromatography ($CHCl_3$/hexane = 1:5) of the residue on silica gel and recrystallization with Et_2O afforded tetracene **2a** (97 mg, 45%) as a yellow solid (m.p. 201–203 °C). **Caution!** Tetracene **2a** in solution was slightly unstable in the presence of both light and air and therefore it should be handled in the dark. In contrast, **2a** in the solid state was stable in the presence of both light and air. ^{1}H NMR (500 MHz, $CDCl_3$): δ = 1.51 [d, J = 6.8 Hz, 24 H, $CH(CH_3)_2$], 3.96 [sept, J = 6.8 Hz, 4 H, $CH(CH_3)_2$], 7.30 (s, 4 H, 2-H, 3-H, 8-H, 9-H), 8.96 (s, 4 H, 5-H, 6-H, 11-H, 12-H) ppm. ^{13}C NMR (126 MHz, $CDCl_3$): δ = 23.59, 28.68, 120.24, 122.86, 128.89, 130.60, 142.28 ppm. MS: m/z (%) = 396 (100) $[M]^+$. $C_{30}H_{36}$ (396.61): calcd. C 90.85, H 9.15; found C 90.53, H 9.11.

1,4,7,10-Tetraisobutyltetracene (2b): This compound was synthesized following the same procedure as described above for **2a** except that reagents **4b** (1.42 g, 7.86 mmol), **5** (1.31 g, 7.86 mmol), KF (430 mg, 7.40 mmol), 18-crown-6 (2.01 g, 7.61 mmol), 10% Pd/C (76 mg), and EtOH (20 mL) were used and the product was purified by column chromatography with $CHCl_3$/hexane (1:1) as eluent. Compound **2b** was formed as a red solid (m.p. 210–212 °C). ^{1}H NMR (500 MHz, $CDCl_3$): δ = 1.06 [d, J = 6.4 Hz, 24 H, $CH_2CH(CH_3)_2$], 2.27–2.31 [m, 4 H, $CH_2CH(CH_3)_2$], 3.07 [d, J = 7.0 Hz, 8 H, $CH_2CH(CH_3)_2$], 7.12 (s, 4 H, 2-H, 3-H, 8-H, 9-H), 8.80 (s, 4 H, 5-H, 6-H, 11-H, 12-H) ppm. ^{13}C NMR (126 MHz, $CDCl_3$): δ = 23.08, 28.73, 43.01, 123.49, 125.19, 128.85, 131.35, 135.69 ppm. MS: m/z (%) = 452 (100) $[M]^+$. $C_{34}H_{44}$ (452.71): calcd. C 90.20, H 9.80; found C 90.07, H 9.79.

1,4,7,10-Tetraisopentyltetracene (2c): This compound was synthesized following the same procedure as described above for **2a** except that reagents **4c** (563 mg, 3.73 mmol), **5** (1.03 g, 1.80 mmol), KF (429 mg, 7.38 mmol), 18-crown-6 (2.01 g, 7.61 mmol), 10% Pd/C (57 mg), and EtOH (20 mL) were used and the product was purified by column chromatography with $CHCl_3$/hexane (1:1) as eluent. Compound **2c** was formed as an orange solid (m.p. 166–168 °C). ^{1}H NMR (500 MHz, $CDCl_3$): δ = 1.08 [d, J = 5.9 Hz, 24 H, $CH_2CH_2CH(CH_3)_2$], 1.76–1.82 [m, 12 H, $CH_2CH_2CH(CH_3)_2$], 3.21 [t, J = 7.6 Hz, 8 H, $CH_2CH_2CH(CH_3)_2$], 7.16 (s, 4 H, 2-H, 3-H, 8-H, 9-H), 8.81 (s, 4 H, 5-H, 6-H, 11-H, 12-H) ppm. ^{13}C NMR (126 MHz, $CDCl_3$): δ = 22.73, 28.35, 31.01, 39.47, 123.24, 123.82, 129.03, 131.03, 136.96 ppm. MS: m/z (%) = 508 (100) $[M]^+$. $C_{38}H_{52}$ (508.82): calcd. C 89.70, H 10.30; found C 89.83, H 10.39.

X-ray Crystallography: Single crystals suitable for X-ray analysis were obtained by slow evaporation from toluene for **2a** and recrystallization from Et_2O for **2b** and **2c**. X-ray data were collected by using a Rigaku/MSC Mercury CCD diffractometer with graphite-monochromated Mo-K_α (λ = 0.7107 Å) radiation at 223 K. The structures were solved by a direct method using SIR2004.[20] All non-hydrogen atoms were anisotropically refined by full-matrix

least-squares on F^2 using SHELXL97.[21] All the hydrogen atoms were geometrically positioned and refined using a riding model with C–H = 0.95, 0.99, 0.99, and 0.98 Å for aromatic, methine, methylene, and methyl carbon atoms, respectively; $U_{iso}(H) = 1.2U_{eq}(C)$ except for methyl H [$1.5U_{eq}(C)$]. All calculations were performed by using the WinGX program package.[22]

Crystal Data for 2a: $C_{30}H_{36}$, M = 396.59, T = 223 K, monoclinic, space group $C2/c$, a = 18.267(8), b = 6.339(2), c = 19.795(8) Å, β = 90.357(2)°, V = 2292.1(16) Å^3, 0.50 × 0.10 × 0.05 mm^3, Z = 4, $\rho_{calcd.}$ = 1.149 g cm^{-3}, μ = 0.064 mm^{-1}, 8113 reflections measured, 2496 unique, 140 parameters refined, GoF = 1.109, $\Delta\rho_{max}$ = 0.23 e Å^{-3}, R_1 = 0.060 {1920 with [$I > 2\sigma(I)$]}, wR = 0.169 (all data).

Crystal Data for 2b: $C_{34}H_{44}$, M = 452.69, T = 223 K, triclinic, space group $P\bar{1}$, a = 5.267(3), b = 11.154(7), c = 11.926(8) Å, α = 85.409(16), β = 84.292(17), γ = 84.952(19)°, V = 692.7(7) Å^3, 0.45 × 0.20 × 0.05 mm^3, Z = 1, $\rho_{calcd.}$ = 1.085 g cm^{-3}, μ = 0.060 mm^{-1}, 5503 reflections measured, 3081 unique, 158 parameters refined, GoF = 1.138, $\Delta\rho_{max}$ = 0.44 e Å^{-3}, R_1 = 0.089 {2612 with [$I > 2\sigma(I)$]}, wR = 0.202 (all data).

Crystal Data for 2c: $C_{38}H_{52}$, M = 508.80, T = 223 K, monoclinic, space group $P2_1/c$, a = 4.809(2), b = 30.304(14), c = 10.973(6) Å, β = 106.366(19)°, V = 1534.3(14) Å^3, 0.25 × 0.03 × 0.03 mm^3, Z = 2, $\rho_{calcd.}$ = 1.101 g cm^{-3}, μ = 0.061 mm^{-1}, 6714 reflections measured, 3501 unique, 176 parameters refined, GoF = 1.005, $\Delta\rho_{max}$ = 0.31 e Å^{-3}, R_1 = 0.121 {1262 with [$I > 2\sigma(I)$]}, wR = 0.291 (all data).

CCDC-746565 (for **2a**), -746563 (for **2b**), and -746564 (for **2c**) contains the supplementary crystallographic data for this paper. These data can be obtained free of charge from The Cambridge Crystallographic Data Centre via www.ccdc.cam.ac.uk/data_request/cif.

Supporting Information (see footnote on the first page of this article): Diverse graphics, ^{1}H and ^{13}C NMR spectra, TD-DFT calculations on **2a**–**c**.

Acknowledgments

This work was supported by the Ministry of Education, Culture, Sports, Science, and Technology (Japan), Grant-in-Aid No. 20550128. We also thank the Instrument Center of the Institute of Molecular Science for X-ray structural analyses, and Chisso Petrochemical Corporation for the gift of reagents.

[1] For reviews see: a) M. Bendikov, F. Wudl, D. F. Perepichka, *Chem. Rev.* **2004**, *104*, 4891–4945; b) J. E. Anthony, *Angew. Chem. Int. Ed.* **2008**, *47*, 452–483.

[2] For selected examples of tetracene derivatives, see: a) A. S. Paraskar, A. R. Reddy, A. Patra, Y. H. Wijsboom, O. Gidron, L. J. W. Shimon, G. Leitus, M. Bendikov, *Chem. Eur. J.* **2008**, *14*, 10639–10647; b) Z. Chen, P. Müller, T. M. Swager, *Org. Lett.* **2006**, *8*, 273–276; c) R. Schmidt, S. Göttling, D. Leusser, D. Stalke, A.-M. Krause, F. Würthner, *J. Mater. Chem.* **2006**, *16*, 3708–3714; d) J. Reichwagen, H. Hopf, A. Del Guerzo, J.-P. Desvergne, H. Bouas-Laurent, *Org. Lett.* **2005**, *7*, 971–974; e) J. A. Merio, C. R. Newman, C. P. Gerlach, T. W. Kelley, D. V. Muyres, S. E. Fritz, M. F. Toney, C. D. Frisbie, *J. Am. Chem. Soc.* **2005**, *127*, 3997–4009; f) S. A. Odom, S. R. Parkin, J. E. Anthony, *Org. Lett.* **2003**, *5*, 4245–4248.

[3] a) C. Kitamura, T. Ohara, N. Kawatsuki, A. Yoneda, T. Kobayashi, H. Naito, T. Komatsu, T. Kitamura, *CrystEngComm* **2007**, *9*, 644–647; b) C. Kitamura, Y. Abe, T. Ohara, A. Yoneda, T. Kawase, T. Kobayashi, H. Naito, T. Komatsu, *Chem. Eur. J.* **2010**, *16*, 880–898.

[4] For the dependence of color on different molecular packing, see: a) G. Klebe, F. Graser, E. Hädicke, J. Berndt, *Acta Crystallogr., Sect. B* **1989**, *45*, 69–77; b) F. Graser, E. Hädicke, *Liebigs Ann. Chem.* **1984**, 483–494; c) F. Graser, E. Hädicke, *Liebigs Ann. Chem.* **1980**, 1994–2011.

[5] a) T. Ozdemir, S. Atilgan, I. Kutuk, L. T. Yildirim, A. Tulek, M. Bayindir, E. U. Akkaya, *Org. Lett.* **2009**, *11*, 2105–2107; b) T. Sato, D.-L. Jiang, T. Aida, *J. Am. Chem. Soc.* **1999**, *121*, 10658–10659.

[6] a) Y. Ooyama, T. Mamura, K. Yoshida, *Eur. J. Org. Chem.* **2007**, 5010–5019; b) Y. Ooyama, S. Yoshikawa, S. Watanabe, K. Yoshida, *Org. Biomol. Chem.* **2006**, *4*, 3406–3409; c) Y. Ooyama, T. Okamoto, T. Yamaguchi, T. Suzuki, A. Hayashi, K. Yoshida, *Chem. Eur. J.* **2006**, *12*, 7827–7838; d) K. Yoshida, Y. Ooyama, H. Miyazaki, S. Watanabe, *J. Chem. Soc. Perkin Trans. 2* **2002**, 700–708.

[7] a) E. Horiguchi, S. Matsumoto, K. Funabiki, M. Matsui, *Bull. Chem. Soc. Jpn.* **2006**, *79*, 799–805; b) E. Horiguchi, S. Matsumoto, K. Funabiki, M. Matsui, *Chem. Lett.* **2004**, *33*, 170–171.

[8] A. Iida, S. Yamaguchi, *Chem. Commun.* **2009**, 3002–3004.

[9] a) A. Wakamiya, K. Mori, S. Yamaguchi, *Angew. Chem. Int. Ed.* **2007**, *46*, 4273–4276; b) C.-H. Zhao, A. Wakamiya, Y. Inukai, S. Yamaguchi, *J. Am. Chem. Soc.* **2006**, *128*, 15934–15935.

[10] Y. Hong, J. W. Y. Lam, B. Z. Tang, *Chem. Commun.* **2009**, 4332–4353.

[11] a) M. Shimizu, H. Tatsumi, K. Mochida, K. Shimono, T. Hiyama, *Chem. Asian J.* **2009**, *4*, 1289–1297; b) M. Shimizu, Y. Takeda, M. Higashi, T. Hiyama, *Angew. Chem. Int. Ed.* **2009**, *48*, 3653–3653.

[12] A. Dreuw, J. Plötner, L. Lorenz, J. Wachtveitl, J. E. Djanhan, J. Brüning, T. Metz, M. Bolte, M. U. Schmidt, *Angew. Chem. Int. Ed.* **2005**, *44*, 7783–7786.

[13] a) Y. Mizobe, T. Hinoue, A. Yamamoto, I. Hisaki, M. Miyata, Y. Hasegawa, N. Tohnai, *Chem. Eur. J.* **2009**, *15*, 8175–8184; b) Y. Mizobe, H. Ito, I. Hisaki, M. Miyata, Y. Hasegawa, N. Tohnai, *Chem. Commun.* **2006**, 2126–2128; c) Y. Mizobe, N. Tohnai, M. Miyata, Y. Hasegawa, *Chem. Commun.* **2005**, 1839–1841.

[14] a) C. Kitamura, C. Matsumoto, N. Kawatsuki, A. Yoneda, K. Asada, T. Kobayashi, H. Naito, *Bull. Chem. Soc. Jpn.* **2008**, *81*, 754–756; b) C. Kitamura, Y. Abe, N. Kawatsuki, A. Yoneda, K. Asada, T. Kobayashi, H. Naito, *Mol. Cryst. Liq. Cryst.* **2007**, *474*, 119–135.

[15] For the photographs of **2a**–**c** in the powder form, see Figure S1 of the Supporting Information.

[16] For details, see the Supporting Information.

[17] a) M. Kasha, *Spectroscopy of the Excited State*, Plenum Press, New York, **1976**; b) M. Kasha, H. R. Rawls, M. Ashraf El-Bayoumi, *Pure Appl. Chem.* **1965**, *11*, 371–392.

[18] J. V. Morris, M. A. Mahaney, J. R. Huber, *J. Phys. Chem.* **1976**, *80*, 969–974.

[19] M. J. Frisch, G. W. Trucks, H. B. Schlegel, G. E. Scuseria, M. A. Robb, J. R. Cheeseman, J. A. Montgomery Jr., T. Vreven, K. N. Kudin, J. C. Burant, J. M. Millam, S. S. Iyengar, J. Tomasi, V. Barone, B. Mennucci, M. Cossi, G. Scalmani, N. Rega, G. A. Petersson, H. Nakatsuji, M. Hada, M. Ehara, K. Toyota, R. Fukuda, J. Hasegawa, M. Ishida, T. Nakajima, Y. Honda, O. Kitao, H. Nakai, M. Klene, X. Li, J. E. Knox, H. P. Hratchian, J. B. Cross, V. Bakken, C. Adamo, J. Jaramillo, R. Gomperts, R. E. Stratmann, O. Yazyev, A. J. Austin, R. Cammi, C. Pomelli, J. W. Ochterski, P. Y. Ayala, K. Morokuma, G. A. Voth, P. Salvador, J. J. Dannenberg, V. G. Zakrzewski, S. Dapprich, A. D. Daniels, M. C. Strain, O. Farkas, D. K. Malick, A. D. Rabuck, K. Raghavachari, J. B. Foresman, J. V. Ortiz, Q. Cui, A. G. Baboul, S. Clifford, J. Cioslowski, B. B. Stefanov, G. Liu, A. Liashenko, P. Piskorz, I. Komaromi, R. L. Martin, D. J. Fox, T. Keith, M. A. Al-Laham, C. Y. Peng, A. Nanayakkara, M. Challacombe, P. M. W. Gill, B. Johnson, W.

Chen, M. W. Wong, C. Gonzalez, J. A. Pople, *Gaussian 03*, *Revision E.01*, Gaussian, Inc., Wallingford, CT, **2004**.
[20] M. C. Burla, R. Caliandro, M. Camalli, B. Carrozzini, G. L. Cascarano, L. De Caro, C. Giacovazzo, G. Polidori, R. Spagna, *J. Appl. Crystallogr.* **2005**, *38*, 381–388.
[21] G. M. Sheldrick, *Acta Crystallogr., Sect. A* **2008**, *64*, 112–122.
[22] L. J. Farrugia, *J. Appl. Crystallogr.* **1999**, *32*, 837–838.
Received: February 18, 2010
Published Online: April 15, 2010

